

Narrow-band tunable terahertz emission from ferrimagnetic $Mn_{3-x}Ga$ thin films

N. Awari, S. Kovalev¹, C. Fowley¹, K. Rode¹, R. A. Gallardo, Y.-C. Lau, D. Betto, N. Thiyagarajah, B. Green, O. Yildirim, J. Lindner, J. Fassbender, J. M. D. Coey, A. M. Deac, and M. Gensch

Citation: *Appl. Phys. Lett.* **109**, 032403 (2016); doi: 10.1063/1.4958855

View online: <http://dx.doi.org/10.1063/1.4958855>

View Table of Contents: <http://aip.scitation.org/toc/apl/109/3>

Published by the [American Institute of Physics](#)

Narrow-band tunable terahertz emission from ferrimagnetic Mn_{3-x}Ga thin films

N. Awari,^{1,2} S. Kovalev,^{1,a)} C. Fowley,^{1,a)} K. Rode,^{3,a)} R. A. Gallardo,⁴ Y.-C. Lau,³ D. Betto,³ N. Thiagarajah,³ B. Green,¹ O. Yildirim,¹ J. Lindner,¹ J. Fassbender,¹ J. M. D. Coey,³ A. M. Deac,¹ and M. Gensch¹

¹Helmholtz-Zentrum Dresden-Rossendorf, Bautzner Landstr. 400, 01328 Dresden, Germany

²University of Groningen, 9747 AG Groningen, Netherlands

³CRANN, AMBER and School of Physics, Trinity College Dublin, Dublin 2, Ireland

⁴Departamento de Física, Universidad Técnica Federico Santa María, Avenida España 1680, 2390123 Valparaíso, Chile

(Received 17 May 2016; accepted 3 July 2016; published online 19 July 2016)

Narrow-band terahertz emission from coherently excited spin precession in metallic ferrimagnetic Mn_{3-x}Ga Heusler alloy nanofilms has been observed. The efficiency of the emission, per nanometer film thickness, is comparable or higher than that of classical laser-driven terahertz sources based on optical rectification. The center frequency of the emission from the films can be tuned precisely via the film composition in the range of 0.20–0.35 THz, making this type of metallic film a candidate for efficient on-chip terahertz emitters. Terahertz emission spectroscopy is furthermore shown to be a sensitive probe of magnetic properties of ultra-thin films. *Published by AIP Publishing.* [<http://dx.doi.org/10.1063/1.4958855>]

Terahertz (THz) emission spectroscopy is a technique based on coherent detection of flashes of THz light emitted when intense ultrashort photon pulses interact with matter. The first demonstration of radiation emitted in this way was in 1990 when it was observed as a result of free carrier excitation and optical rectification in semiconductors.¹ The emitted pulses were broadband, single-cycle THz transients. The emission spectrum is governed by the laser pulse duration, carrier relaxation time, phonon absorption, and/or the electro-optical coefficients.

Since then, a multitude of materials has been investigated with the aim of increasing the efficiency of THz generation and optimizing the emission spectrum. In 2004, it was discovered that laser-driven demagnetization processes can give rise to broadband, single-cycle THz pulse emission.^{2,3} In that case, the spectrum of the emitted burst carries information on the time-scale of the demagnetization process, making THz emission spectroscopy a powerful diagnostic technique for studying laser-driven non-equilibrium dynamics in matter. Then, in 2013, the method was successfully applied to determine the duration of ultra-fast laser-driven spin currents.⁴ Most recently, two groups have succeeded in detecting narrow-band emission from spin waves in ferrimagnetic bulk insulators.^{5,6}

In this letter, we report on the observation of narrow-band laser-driven emission from ultra-thin, metallic, ferrimagnetic films. Furthermore, we demonstrate that THz emission spectroscopy is a competitive technique to measure magnetic properties of ultra-thin films.

The samples studied belong to the D_{022} class of tetragonal Mn-rich Heusler alloys Mn_{3-x}Ga ,^{7–10} which have recently attracted considerable attention due to their unique combination of low saturation magnetization, high spin polarization,

high magneto-crystalline anisotropy, and low magnetic damping.^{11–13} In Mn_{3-x}Ga , these properties are easily tuned by varying the Mn content, which modifies the center frequency of the narrow-band THz emission via the sublattice magnetizations and anisotropies.

Our experimental set-up is shown in Figure 1(a). The samples are irradiated at normal incidence with unfocused pulses from a laser-amplifier system with a wavelength of 800 nm and a repetition rate of 1 kHz. The laser pulse duration of 100 fs is much shorter than the period of the emitted THz bursts enabling fully coherent emission. The emitted radiation is detected in the backward direction. Our detection principle for the emitted light pulses is based on electro-optic sampling in a 2 mm thick ZnTe crystal;¹⁴ a small portion of the excitation pulses is split-off by a dichroic mirror (DM) acting as a 1:1000 beam splitter. Electro-optical detection enables the removal of any thermal background from the measurement and hence allows extremely weak pulses to be observed. Our frequency range is limited to below 2 THz by the phase matching between THz and near infrared (NIR) laser wavelengths in the ZnTe crystal. All measurements were done in ambient conditions.

Thin films of three different alloy compositions— Mn_2Ga , $\text{Mn}_{2.5}\text{Ga}$, and Mn_3Ga —were grown by magnetron sputtering on heated MgO substrates in a fully automated “Shamrock” deposition tool with a base pressure of 1×10^{-8} Torr; the optimal deposition temperature of the substrate was found to be 350 °C. Mn_3Ga and Mn_2Ga samples were grown from stoichiometric targets at a power of 30 W for 40 min, while $\text{Mn}_{2.5}\text{Ga}$ was grown by co-sputtering from the Mn_3Ga and the Mn_2Ga targets at equal power of 20 W for 30 min.^{7,10} The crystal structure was determined by X-ray diffraction. All three films crystallize in the tetragonal D_{022} structure (space group 139), illustrated in Fig. 1(b). Mn in the 4d positions, couples ferromagnetically to each other, while the 4d and 2b magnetic sublattices are strongly antiferromagnetically

^{a)}Authors to whom correspondence should be addressed. Electronic addresses: s.kovalev@hzdr.de; c.fowley@hzdr.de; and rodek@tcd.ie

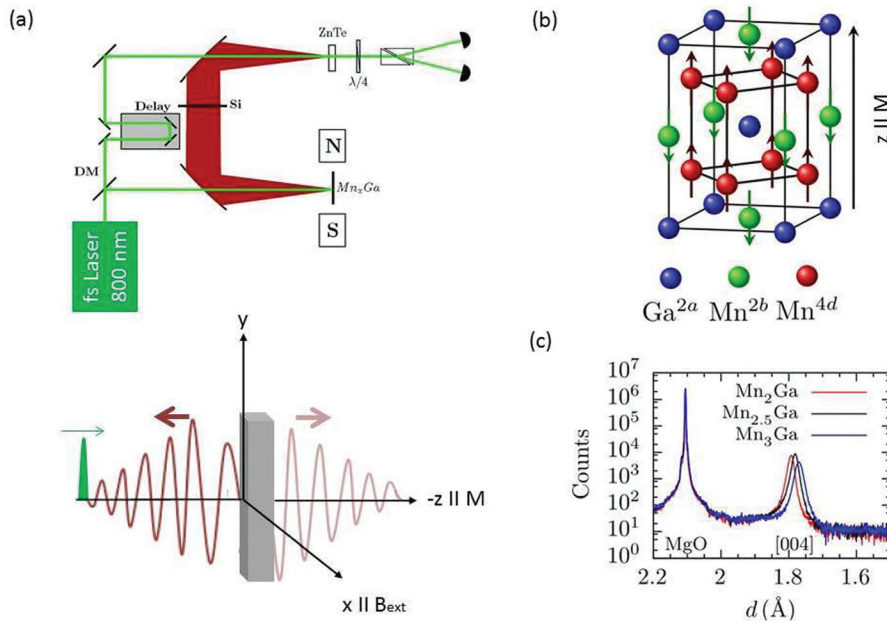


FIG. 1. (a) Schematic of the THz emission spectroscopy set-up (top) and sample geometry employed for the Mn_{3-x}Ga samples (bottom). (b) Idealized crystal structure of Mn_3Ga . The arrows represent the magnetic moment on each Mn site. The crystallographic c -axis is perpendicular to the sample surface and parallel to the net magnetic moment. (c) X-ray diffraction of Mn_{3-x}Ga samples showing the lattice parameter varying from 7.08 to 7.17 Å with increasing x .

coupled, resulting in ferrimagnetic order. For the stoichiometric compound ($x=0$), the net moment per formula unit is $2|m^{4d}| - |m^{2b}|$. The local symmetry, especially the Ga coordination of the two Mn-sites is quite different, leading to different magnetic properties for the Mn on the two different sites.

Mn in $2b$ positions possesses a larger magnetic moment of $\sim 3.3 \mu_B$ with weak easy- c -plane anisotropy ($K_u = -0.09 \text{ MJ m}^{-3}$), while the Mn in $4d$ positions has a smaller moment of $\sim 2.1 \mu_B$ and strong easy- c -axis anisotropy ($K_u = 2.26 \text{ MJ m}^{-3}$).⁹ As the composition of the films is varied from $x=0$ to 1 (from Mn_3Ga to Mn_2Ga), Mn is primarily lost from the $2b$ position. Hence, the net magnetization increases with increasing x , and there is no compensation composition. Simultaneously, ions with in-plane anisotropy are replaced by vacancies, so that the net magnetocrystalline anisotropy increases.

Saturation magnetization (M_s) and coercivity ($\mu_0 H_c$) were determined by vibrating sample magnetometry (VSM). However, the magnetic anisotropy field, $\mu_0 H_k$, exceeds the field available in our magnetometer, so it was not possible to saturate the magnetization in the plane of the films. $\mu_0 H_k$ is usually determined by extrapolation,¹⁵ but other techniques such as anomalous Hall effect,¹⁶ electron spin resonance (ESR),¹⁷ or dynamic all-optical MOKE/Faraday measurements¹¹ can also be used. The two latter methods relate the resonance frequency to the magnetic properties via the Kittel formula.¹⁸

In ferrimagnetic materials, where the two sublattices have different magnetizations and anisotropies but are strongly coupled to each other by exchange, one expects two fundamental modes: one where the two sublattices precess out-of-phase and one where they remain in-phase. Due to the antiferromagnetic exchange coupling, we expect the out-of-phase mode to have lower energy and frequency. Describing the ferrimagnet as a system of two exchange-coupled ferromagnetic layers an expression relating the out-of-phase mode to the properties of each sublattice can be derived at zero external field (see [supplementary material](#) for details)

$$f_{\text{res}} = (\gamma_{\text{eff}}/2\pi)(\mu_0 H_k - \mu_0 M_s), \quad (1)$$

where γ_{eff} is an effective value of the gyromagnetic ratio, $\mu_0 H_k$ is an effective perpendicular anisotropy field, which depends on the sub-lattice anisotropy and magnetizations of both sublattices. M_s is the net saturation magnetization ($M_{4d} - M_{2b}$). These values and hence the resonance frequency can be controlled via the films' stoichiometry. Using previously obtained data from neutron scattering measurements on bulk Mn_3Ga samples,⁹ the frequency of the out-of-phase mode in Mn_3Ga is predicted from Eq. (1), to lie in the region of 0.35 THz. This is at the same time the highest frequency expected in Mn_{3-x}Ga thin films. Due to the loss of Mn from the $2b$ sites when $x=1$, the lowest frequency should be observed for Mn_2Ga . Assuming that the Mn on the $2b$ sites is completely lost, the low frequency limit is estimated to be 0.12 THz. The frequency tunability is limited in both directions by the eventual loss of the tetragonal D_{022} structural phase. Note that the in-phase mode, due to the extremely large exchange fields in the system, should exhibit higher frequencies which could reach values in excess of 4 THz in Mn_3Ga .

The process of THz emission from coherent spin precession can be understood as follows. The 100 fs NIR laser pulse leads to both ultrafast demagnetization and a sudden change of the easy axis of the magnetic system.¹⁹ This in turn produces a coherent precessional motion of the net magnetization \mathbf{M} around the easy axis with a frequency $f_{\text{res,exc}}$ that converges towards the frequency f_{res} given in Eq. (1) for low excitation fluences. In the case of strong, easy- c -axis, magnetocrystalline anisotropy, the tip of the magnetization vector oscillates around the crystallographic c -axis, corresponding to the x - y plane in our experimental geometry shown in Fig. 1. A small external field is applied in the x -direction in order to synchronize the precession of the spins after the ultra-fast perturbation allowing for the emission of a coherent wave. The emitted electric field due to both demagnetization and spin precession can be expressed as^{6,20,21}

$$\mathbf{E} \sim d^2/dt^2(\mu_0 \mathbf{M}). \quad (2)$$

As can be seen from Eq. (2), it is proportional to the second derivative of M . This implies the following: the electric field vector of the wave originating from the precession of the out-of-phase mode is oriented perpendicular to M and lies in the $(x-y)$ plane. This wave therefore propagates in the z direction, normal to the film surface, and the electric field component along the y -axis is

$$E_y \sim A_0 e^{-\delta t} \sin(2\pi f_{\text{res,dyn}} t), \quad (3)$$

where A_0 is the initial deflection of M caused by the laser excitation and δ is the damping of the precessional motion. It is interesting to note that THz emission spectroscopy probes the in-plane components, making it complementary to Faraday effect measurements, which probe the out-of-plane component.

THz emission measurements for the three different compositions are shown in Fig. 2. The laser excitation fluence in all measurements was 0.1 mJ cm^{-2} . The observed center frequency depends on composition and shifts from 0.205 THz for Mn_2Ga to 0.352 THz for Mn_3Ga . The frequency resolution in the intensity spectra shown in Fig. 2 is defined by the time-window in the time-domain measurements and does not represent the natural bandwidth of the emission (see [supplementary material](#) for details). The phase of the emitted coherent THz transient can be reversed by the sign of an

in-plane external magnetic field (see inset of Figure 2(a)) proving that the emission is of magnetic origin. We estimate the resonance frequency f_{res} under equilibrium conditions from a detailed analysis of the effect of excitation fluence (Fig. 3(a)). The center frequencies are determined, for each excitation fluence, by fitting a damped sine function to the measurements (see [supplementary material](#) for details). Below 0.5 mJ cm^{-2} , the resonant frequency decreases linearly with increasing fluence. Even the comparatively moderate fluence of 0.1 mJ cm^{-2} leads to a lowering of the observed “dynamic” center frequency $f_{\text{res,dyn}}$ possibly due to heating. The extrapolated frequency at zero excitation will be used as an approximation for f_{res} at equilibrium (see Table I). Another approach that allows direct measurement of the quasi-equilibrium frequency is THz-driven transient Faraday probe measurements, where the magnetic field of the THz pulse couples directly to the spins via the Zeeman-torque.²² We were able to drive the same mode in the Mn_3Ga film selectively by resonant THz excitation. The spectral densities, orders of magnitude higher than those available from tabletop sources,²³ made it possible to detect the minute Faraday rotation signal (green solid line, Fig. 2(c)). The absorbed energy goes predominantly into excitation of the coherent spin precession, so that heating and off-resonant excitation is minimal. The derived frequencies should therefore

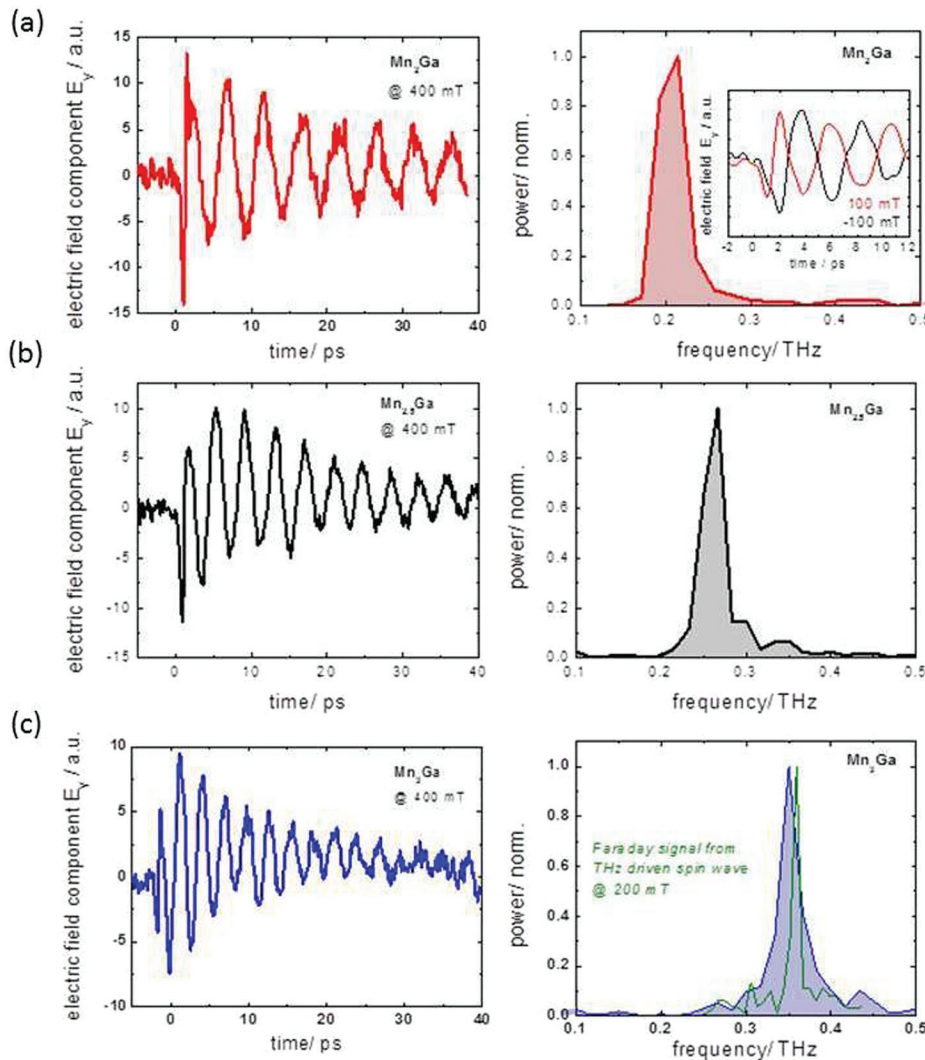


FIG. 2. THz emission spectroscopy measurements. The detected THz waveform is shown on the left and the corresponding spectrum obtained by Fourier transformation is shown on the right for (a) 45 nm Mn_2Ga , (b) 65 nm $\text{Mn}_{2.5}\text{Ga}$ and (c) 46 nm thick Mn_3Ga films. All measurements were performed with a moderate laser fluence of 0.1 mJ cm^{-2} and in a small external magnetic field ranging from 100 to 400 mT, oriented parallel to the sample surface, along the x -axis. The inset of (a) shows the time-domain waveforms for an applied field of 100 mT, directed along $+x$ and $-x$, respectively. The phase shift between the two is 180° , proving their magnetic origin. Also shown in (c) is a Faraday measurement of the resonance driven by direct THz excitation with an intense quasi-cw narrow-band THz source²³ (green solid line).

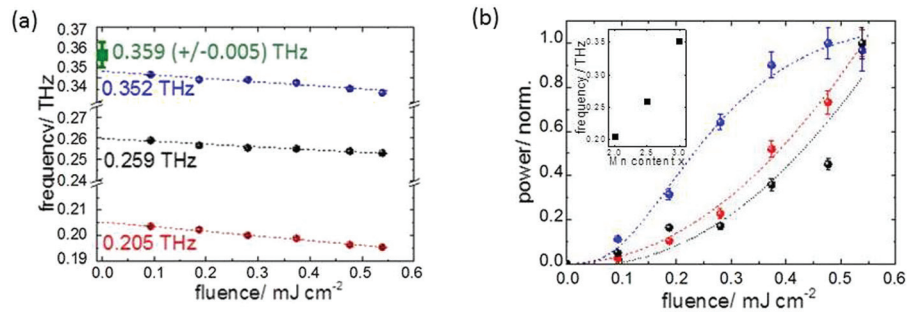


FIG. 3. (a) Fluence dependence of the center frequency (red, Mn_2Ga ; black, $\text{Mn}_{2.5}\text{Ga}$; and blue, Mn_3Ga). At low fluences the dependence is linear. Equilibrium values for f_{res} are determined from the intercept with the frequency axis. All measurements were performed at 19.5°C in a horizontal field of 400 mT applied parallel to the sample surface along the x -direction. The FM mode frequency derived for Mn_3Ga via THz driven Faraday rotation measurements in a 200 mT field is also shown (green). (b) Fluence dependence of the emitted THz power normalized to a fluence of 0.54 mJ cm^{-2} . Mn_2Ga (red) and $\text{Mn}_{2.5}\text{Ga}$ (black) show the expected quadratic dependence while Mn_3Ga (blue) seems to already reach saturation at a fluence of 0.5 mJ cm^{-2} . (Inset) Center frequency as a function of Mn content.

correspond better to the equilibrium value. We find that the frequency derived from THz-driven transient Faraday rotation is slightly higher than the value inferred from linear extrapolation of the emission measurements, in qualitative agreement with the above discussion.

Although ferrimagnetic materials like Mn_{3-x}Ga should exhibit two different fundamental magnetic modes, we have only been able to observe emission from the lower-frequency, out-of-phase mode. In Table I, we give the effective anisotropy field as observed by THz emission, calculated using Eq. (1), M_s and f_{res} . The derived values range from roughly 8 T for Mn_2Ga to 13 T for Mn_3Ga in good agreement with literature values.^{7,10}

Most laser-based sources in the lower THz frequency range are broadband emitters. The narrow bandwidth and the tunability of the center frequencies make Mn_{3-x}Ga films an interesting alternative. Assuming that the emitted THz field is proportional to the initial laser-induced deflection of \mathbf{M} , the emitted THz power should scale with the square of the excitation fluence. At high fluences, one expects to reach saturation, due to heating and subsequent loss of magnetization. In Fig. 3(b), we show the normalized emission power as a function of the excitation fluence. Quadratic behavior is

TABLE I. M_s from VSM and inferred values of $\mu_0 H_k$ from dynamic THz emission measurements. The comparison of the emitted THz power per nanometer film thickness normalized to ZnTe and results from a THz driven Faraday rotation measurements are also shown. THz emission measurements have been performed in the presence of an external magnetic field of 400 mT and at a temperature of 19.5°C . THz driven Faraday rotation measurements were performed with an external magnetic field of 200 mT.

	Mn_2Ga	$\text{Mn}_{2.5}\text{Ga}$	Mn_3Ga
Magnetometry			
$\mu_0 M_s$ (T)	0.401	0.263	0.163
NIR-driven THz emission			
Observed f_{res} (THz)	0.205	0.259	0.352
Bandwidth Δf_{res} (THz)	0.012	0.018	0.029
$\mu_0 H_k$ (T)	7.98	9.95	13.17
Power ^{1/2} /nm (norm. to ZnTe)	8	9	5.7
THz-driven transient Faraday rotation			
Observed f_{res} (THz)	0.359 ± 0.005
$\mu_0 H_k$ (T)	13.43

indeed observed for Mn_2Ga and $\text{Mn}_{2.5}\text{Ga}$, but emission from Mn_3Ga seems to reach saturation as early as 0.5 mJ cm^{-2} .

In order to compare the efficiency of the emission to existing THz emitters, the emission of the Mn_{3-x}Ga samples has been measured at a fluence of 0.5 mJ cm^{-2} , one after the other followed by a measurement of the emission of a $100 \mu\text{m}$ thick ZnTe crystal. We find that the Mn_{3-x}Ga emission per nanometer film thickness exceeds that of ZnTe in their respective narrow frequency band (Table I), by a factor of almost ten. Due to the pulsed nature of the excitation and the very thin films, the emitted average power is too low to be measured directly. It can however be approximated from the sampled electric field transients. We find for all the investigated Mn_{3-x}Ga films average powers in range of few hundred femtowatt (fW) to a few picowatt (pW). At the present stage, no clear systematic correlation between the film stoichiometry or deposition conditions and the emitted THz power could be found that would allow to speculate on how the THz emission can be optimized by the growth parameters. However, optimizing the emitter geometry by, for example, growing multi-layer stacks of nanofilms would potentially increase the output power by orders of magnitude, as has been shown for stacks of intrinsic Josephson junction emitters.²⁴

To summarize, we have demonstrated narrow-band THz emission from an ultra-thin, ferrimagnetic metallic film. The observed bandwidth of the emission is between 6% and 9% and hence considerably larger than the one found for low temperature intrinsic Josephson junctions THz emitters²⁴ which operate in a similar frequency range. The emission frequency can be tuned via the Mn-content, in agreement with earlier work based on transient Kerr measurements.¹¹ The efficiency of this type of spintronic emission is, within the narrow emission bandwidth, comparable or even up to an order of magnitude greater than that of classical ZnTe emitters based on optical rectification.²⁵ This makes Mn_{3-x}Ga thin films interesting candidates for narrow-band, on-chip, spintronic emitters in the sub-THz frequency range. Heusler-type alloys may furthermore be integrated as free layers in spin-transfer-torque driven oscillators.^{26,27} This could propel such devices into the terahertz regime, combining the high tunability and output power of spin-torque oscillators²⁸ with the ultra-high frequency intrinsic to the materials analyzed here. Further increase of the resonance frequencies may be achieved by alloying different tetragonal Heuslers or by atomic substitution.^{29,30}

In order to derive quantitative values of the sublattice anisotropies, magnetizations, and interlayer exchange field, an extensive analysis of the field dependence of the frequency is required. THz emission spectroscopy is complementary to neutron scattering as it provides the sensitivity to investigate films only a few nanometer thick. It is closely related to all-optical, time-resolved Kerr/Faraday effect measurements and provides access to in-plane magnetization components during precession.

Our work opens the prospect of applying THz emission spectroscopy as a routine analytical tool for determining equilibrium magnetic properties. To this end, direct, selective, coherent THz excitation of the fundamental magnetic resonances may be a crucial next development.^{5,22,23}

See [supplementary material](#) for more detailed information on: (i) the theoretical description of the ferrimagnetic system by means of two exchange coupled ferromagnetic sub-lattices and (ii) the analysis of the experimentally derived THz emission data.

N.A. acknowledges support through the Ubbo Emmius Program of the University of Groningen. K.R., Y.C.L., D.B., N.T., and J.M.D.C. acknowledge the funding by the SFI through AMBER and Grant No. 13/ERC/12561. D.B. acknowledges funding through IRCSET. O.Y. would like to thank Dr. S. Zhou (HZDR) for the access and assistance to the VSM. R.A.G. acknowledges the financial support from CONICYT PAI/ACADEMIA, under Contract No. 79140033. C.F., O.Y., and A.M.D. acknowledge support by Helmholtz Young Investigator Initiative Grant No. VH-N6-1048.

¹X. C. Zhang, X. C. Zhang, B. B. Hu, J. T. Darrow, and D. H. Auston, "Generation and femtosecond electromagnetic pulses from semiconductor surfaces," *Appl. Phys. Lett.* **56**, 1011 (1990).

²E. Beaurepaire, G. M. Turner, S. M. Harrel, M. C. Beard, J.-Y. Bigot, and C. A. Schmuttenmaer, "Coherent terahertz emission from ferromagnetic films excited by femtosecond laser pulses," *Appl. Phys. Lett.* **84**, 3465 (2004).

³D. J. Hilton, R. D. Averitt, C. A. Meserole, G. L. Fisher, D. J. Funk, J. D. Thompson, and A. J. Taylor, "Terahertz emission via ultrashort-pulse excitation of magnetic metal films," *Opt. Lett.* **29**, 1805 (2004).

⁴T. Kampfrath, M. Battiato, P. Maldonado, G. Eilers, J. Nötzold, S. Mährlein, V. Zbarsky, F. Freimuth, Y. Mokrousov, and S. Blügel, "Terahertz spin current pulses controlled by magnetic heterostructures," *Nat. Nano.* **8**, 256 (2013).

⁵T. H. Kim, S. Y. Hamh, J. W. Ham, C. Kang, C.-S. Kee, S. Jung, J. Park, Y. Tokunaga, Y. Tokura, and J. S. Lee, "Coherently controlled spin precession in canted antiferromagnetic YFeO₃ using terahertz magnetic field," *Appl. Phys. Exp.* **7**, 093007 (2014).

⁶Z. Jin, Z. Mics, G. Ma, Z. Cheng, M. Bonn, and D. Turchinovich, "Single-pulse terahertz coherent control of spin resonance in the canted antiferromagnet YFeO₃, mediated by dielectric anisotropy," *Phys. Rev. B* **87**, 094422 (2013).

⁷H. Kurt, K. Rode, M. Venkatesan, P. Stamenov, and J. M. D. Coey, "High spin polarization in epitaxial films of ferrimagnetic Mn₃Ga," *Phys. Rev. B* **83**, 020405 (2011).

⁸H. Kurt, K. Rode, H. Tokuc, P. Stamenov, M. Venkatesan, and J. M. D. Coey, "Exchange-biased magnetic tunnel junctions with antiferromagnetic-Mn₃Ga," *Appl. Phys. Lett.* **101**, 232402 (2012).

⁹K. Rode, N. Baadji, D. Betto, Y.-C. Lau, H. Kurt, M. Venkatesan, P. Stamenov, S. Sanvito, J. M. D. Coey, E. Fonda et al., "Site-specific order

and magnetism in tetragonal Mn₃Ga thin films," *Phys. Rev. B* **87**, 184429 (2013).

¹⁰H. Kurt, K. Rode, M. Venkatesan, P. Stamenov, and J. M. D. Coey, "Mn_{3-x}Ga (0 ≤ x ≤ 1): Multifunctional thin film materials for spintronics and magnetic recording," *Phys. Status Solidi B* **248**, 2338 (2011).

¹¹S. Mizukami, F. Wu, A. Sakuma, J. Walowski, D. Watanabe, T. Kubota, X. Zhang, H. Naganuma, M. Oogane, Y. Ando, and T. Miyazaki, "Long-lived ultrafast spin precession in manganese alloys films with a large perpendicular magnetic anisotropy," *Phys. Rev. Lett.* **106**, 117201 (2011).

¹²S. Mizukami, A. Sugihara, S. Iihama, Y. Sasaki, K. Z. Suzuki, and T. Miyazaki, "Laser-induced THz magnetization precession for a tetragonal Heusler-like nearly compensated ferrimagnet," *Appl. Phys. Lett.* **108**, 012404 (2016).

¹³G. Kreiner, A. Kalache, S. Hausdorf, V. Alijani, J.-F. Qian, G. Shan, U. Burkhardt, S. Ouardi, and C. Felser, "New Mn₂-based Heusler compounds," *Z. Anorg. Org. Chem.* **640**, 783 (2014).

¹⁴G. Gallot and D. Grischkovsky, "Electro-optic detection of terahertz radiation," *J. Opt. Soc. Am. B* **16**, 1204 (1999).

¹⁵M. Glas, D. Ebke, I.-M. Imort, P. Thomas, and G. Reiss, "Anomalous Hall effect in perpendicularly magnetized Mn_{3-x}Ga thin films," *JMMM* **333**, 134 (2013).

¹⁶C. Fowley, S. Ouardi, T. Kubota, O. Yildirim, A. Neudert, K. Lenz, V. Sluka, J. Lindner, J. M. Law, S. Mizukami et al., "Direct measurement of the magnetic anisotropy field in Mn-Ga and Mn-Co-Ga Heusler films," *J. Phys. D: Appl. Phys.* **48**, 164006 (2015).

¹⁷A. N. Ponomaryov, M. Ozerov, L. Zviagina, J. Wosnitza, K. Yu. Povarov, F. Xiao, A. Zheludev, C. Landee, E. Čížmár, A. A. Zvyagin, and S. A. Zvyagin, "Electron spin resonance in a strong-rung spin-12 Heisenberg ladder," *Phys. Rev. B* **93**, 134416 (2016).

¹⁸A. G. Gurevich and G. A. Melkov *Magnetization Oscillations and Waves* (CRC Press/Taylor and Francis Group, 1996).

¹⁹M. van Kampen, C. Jozsa, J. T. Kohlhepp, P. LeClair, L. Lagae, W. J. M. de Jonge, and B. Koopmans, "All-optical probe of coherent spin waves," *Phys. Rev. Lett.* **88**, 227201 (2002).

²⁰G. Song, Z. Jin, X. Lin, J. Jiang, X. Wang, H. Wu, G. Ma, and S. Cao, "The polarization trajectory of terahertz magnetic dipole transition in (100)-oriented PrFeO₃ single crystal," *J. Appl. Phys.* **115**, 163108 (2014).

²¹D. J. Hilton, R. P. Prasankumar, S. A. Trugman, A. J. Taylor, and R. D. Averitt, "On photo-induced phenomena in complex materials probing quasi-particle dynamics using infrared and far-infrared pulses," *J. Phys. Soc. Jpn.* **75**, 011006 (2006).

²²T. Kampfrath, A. Sell, G. Klatt, A. Pashkin, S. Mährlein, T. Dekorsy, M. Wolf, M. Fiebig, A. Leitenstorfer, and R. Huber, "Coherent THz control of antiferromagnetic spin waves," *Nature Photon.* **5**, 31 (2011).

²³B. Green, S. Kovalev, V. Asgekar, G. Geloni, U. Lehnert, T. Goltz, M. Kuntzsch, C. Bauer, J. Hauser, and J. Voigtlaender, "High-field high-repetition-rate sources for coherent THz control of matter," *Sci. Rep.* **6**, 22256 (2016).

²⁴U. Welp, K. Kadowaki, and R. Kleiner, "Superconducting emitters of THz radiation," *Nature Photon.* **7**, 702 (2013).

²⁵M. C. Hoffmann and J. Fülöp, "Intense ultrashort terahertz pulses: Generation and applications," *J. Phys. D* **44**, 083001 (2011).

²⁶M. Zic, K. Rode, N. Thiyagarajah, Y.-C. Lau, D. Betto, J. M. D. Coey, S. Sanvito, K. J. O'Shea, C. A. Ferguson, and D. A. MacLaren, "Designing a fully compensated half-metallic ferrimagnet," *Phys. Rev. B* **93**, 140202(R) (2016).

²⁷K. Borisov, D. Betto, Y.-C. Lau, C. Fowley, A. Titova, N. Thiyagarajah, G. Atcheson, J. Lindner, A. M. Deac, J. M. D. Coey et al., "Tunnelling magnetoresistance of the half-metallic compensated ferrimagnet Mn₂RuGa," *Appl. Phys. Lett.* **108**, 192407 (2016).

²⁸A. M. Deac, A. Fukushima, H. I. Kubota, H. Maehara, Y. Suzuki, S. Yuasa, Y. Nagamine, K. Tsunekawa, D. D. Djayaprawira, and N. Watanabe, "Bias-driven high-power microwave emission from MgO-based tunnel magnetoresistance devices," *Nat. Phys.* **4**, 803 (2008).

²⁹H. Kurt, K. Rode, P. Stamenov, M. Venkatesan, Y.-C. Lau, E. Fonda, and J. M. D. Coey, "Cubic Mn₂Ga thin films: Crossing the spin gap with ruthenium," *Phys. Rev. Lett.* **112**, 027201 (2014).

³⁰T. Graf, C. Felser, and S. S. P. Parkin, "Simple rules for the understanding of Heusler compounds," *Prog. Solidi Status Chem.* **39**, 1 (2011).